Pedosphere **36**(2): 540–553, 2026
doi: 10.1016/j.pedsph.2024.11.003
ISSN 1002-0160/CN 32-1315/P

Published by Elsevier B.V. and Science Press

PEDOSPHERE

www.elsevier.com/locate/pedosphere

Arbuscular mycorrhizal symbiosis enhances microbial contribution to mineral-associated organic carbon persistence in soil: Insights from soil microbial community and microbial necromass carbon

Yin LIU[1,2], Jin QIAN[1,2,*], Yueming ZHU[3], Jing HU[4], Bianhe LU[1,2], Yuxuan HE[1,2] and Junwei SHEN[1,2]

[1]*Key Laboratory of Integrated Regulation and Resource Development on Shallow Lakes, Ministry of Education, Hohai University, Nanjing 210098 (China)*
[2]*College of Environment, Hohai University, Nanjing 210098 (China)*
[3]*Nanjing Institute of Environmental Sciences, Ministry of Ecology and Environment, Nanjing 210042 (China)*
[4]*Department of Civil, Environmental and Construction Engineering, University of Central Florida, Orlando FL 32816 (USA)*

(Received June 27, 2024; revised August 25, 2024; accepted October 29, 2024)

ABSTRACT

The formation of mineral-associated organic carbon (MAOC), a critical soil fraction related to soil organic carbon (SOC) sequestration, is significantly influenced by microbial processes. Yet, how arbuscular mycorrhizal (AM) symbiosis impacts MAOC accumulation in rhizosphere soils through its effects on microbial contribution remains poorly understood. Here, a pot experiment was conducted in a climate chamber using *Lythrum salicaria* L. as the host plant and *Archaeospora trappei* as the AM fungi inoculum to assess the microbial community in the samples collected from bulk soil (BS) and rhizosphere soil (RS) under the AM fungi inoculation (+AM) and non-inoculation (−AM) treatments using 16S rRNA sequencing. The results showed that AM symbiosis influenced soil microbial community composition and enhanced soil microbial community functions related to carbon (C) degradation. The number of live and dead cells (all cells in the soil) was the highest in RS under the +AM treatment (RS+AM) based on confocal laser scanning microscopy images. Meanwhile, AM symbiosis increased the proportions of apoptotic cells (19.02%) and necrotic cells (12.12%) in RS. Using soil amino sugars as microbial biomarkers, the concentrations of bacterial necromass C (188.01 g kg^{-1} OC) and fungal necromass C (392.19 g kg^{-1} OC) were the highest in the MAOC fraction in RS+AM. Additionally, the MAOC content (17.20 g kg^{-1} soil) and proportion (42.06%) were the highest in RS+AM. This study illustrated two primary mechanisms by which AM symbiosis enhanced MAOC accumulation: 1) altering soil microbial community composition and functions related to C degradation and 2) promoting the input of microbial necromass C, especially fungal necromass C. This study broadens our horizons to understand the mechanisms of microbial contribution to MAOC accumulation stimulated by AM symbiosis in rhizosphere soils and provides management practices for the application of AM fungi to SOC sequestration.

Key Words: arbuscular mycorrhizal fungi, carbon sequestration, fungal necromass carbon, microbial community function, soil carbon degradation, soil organic carbon

Citation: Liu Y, Qian J, Zhu Y M, Hu J, Lu B H, He Y X, Shen J W. 2026. Arbuscular mycorrhizal symbiosis enhances microbial contribution to mineral-associated organic carbon persistence in soil: Insights from soil microbial community and microbial necromass carbon. *Pedosphere*. **36**(2): 540–553.

INTRODUCTION

Soil organic carbon (SOC), as the largest carbon (C) pool in terrestrial ecosystems, is recognized to play a critical role in C storage and management to address the challenges of global climate change (Cotrufo *et al*., 2015; Lugato *et al*., 2021; Terrer *et al*., 2021; Wang Z G *et al*., 2023). To predict SOC dynamics and vulnerability more accurately, SOC is separated into two different fractions in function, particulate organic carbon (POC) and mineral-associated organic carbon (MAOC) (Cotrufo *et al*., 2019; Lavallee *et al*., 2020). Compared to POC, MAOC is less accessible to microbial decomposition and exhibits higher levels of stability and persistence in soil (Kleber *et al*., 2015; Heckman *et al*., 2023). A multitude of biological and biochemical factors influence the formation and cycling of POC and MAOC, including plant root exudates, arbuscular mycorrhizal fungi (AMF), and soil microbial physiological traits (Sokol *et al*., 2019; Li *et al*., 2021; Yin *et al*., 2021; Chari and Taylor, 2022). In the rhizosphere, AMF can form symbiotic associations with roots and affect soil C dynamics and sequestration by inducing greater root C allocation and promoting the rhizosphere priming effect (Olsson *et al*., 2010; van der Heijden *et al*., 2015). Though the positive effects of arbuscular mycorrhizal (AM) symbiosis on soil C sequestration and MAOC accumulation have been widely recognized in various ecosystems (Averill *et al*., 2014; Bai and Cotrufo, 2022), the influence of the rhizosphere microbial process induced by AM symbiosis on MAOC distribution remains poorly elucidated. Furthermore, wetlands play a crucial role in storing 20%–30% of global soil C, possessing a significant and undeniable C sequestration capacity (Nahlik and Fennessy, 2016; Wang *et al*.,

*Corresponding author. E-mail: hhuqj@hhu.edu.cn.

2019). However, the knowledge of the distribution of POC and MAOC in wetland ecosystems under the effect of AMF is relatively scarce.

At the global scale, soil microbial necromass (*i.e*., dead microbial cells and their degradants) not only makes up a large portion of SOC, but also constitutes a crucial source of MAOC (Wang B R *et al*., 2021a; Wang C *et al*., 2021; Zhang Z L *et al*., 2022). Despite the fact that aboveground plant inputs (fast-decaying plant litter) enhance the SOC content in temperate forests, this phenomenon can not be explained by microbial necromass (Craig *et al*., 2022). Instead, the increase of belowground plant inputs can facilitate microbial necromass contribution to SOC storage in terrestrial ecosystems, such as grasslands, croplands, and forests (Lange *et al*., 2015; Liang *et al*., 2019; Bai and Cotrufo, 2022; Camenzind *et al*., 2023). Moreover, a portion of belowground plant inputs (root-derived organic inputs) could undergo decomposition and conversion into microbial necromass, which subsequently gets stabilized on mineral surfaces and eventually contributes to the build-up of the MAOC pool in ecosystems (Cotrufo *et al*., 2013; Heckman *et al*., 2023). Thus, in order to improve our comprehension and prediction of SOC sequestration and stabilization, it is of utmost importance to explore the impacts of microbial necromass generated from plant-derived inputs on the MAOC content from the perspective of the rhizosphere environment.

Fungal and bacterial necromass together constitute microbial necromass; however, there are distinct differences in the formation and turnover processes between fungal and bacterial necromass (Liang *et al*., 2019). Compared to bacteria, fungi form more macromolecular aggregations with thicker cell walls and hyphae, and the stabilization of fungal necromass in soil is more efficient through the interaction with the tannin complex (Adamczyk *et al*., 2019; Wang B R *et al*., 2021a). Throughout the decomposition process, fungal and bacterial necromass contribute differently to SOC accumulation depending on the associated microbial community (Xue *et al*., 2024). Notably, it has been shown that fungal necromass contributes more to SOC in comparison to bacterial necromass at different soil depths as well as in several ecosystems (grassland, arable land, and forest) consistently (Joergensen, 2018; Li *et al*., 2022; Lv *et al*., 2022). However, the difference in the contribution of bacterial and fungal necromass to the formation of MAOC fraction in the rhizosphere is uncertain. Moreover, AM fungal necromass could contribute more to soil C storage than ectomycorrhizal fungal biomass, because the fraction of acid-hydrolyzable material is significantly greater in AMF (Kuyper and Jansa, 2023). It has been reported that the extraradical mycelium of AMF beyond the rhizosphere also contributes to the accumulation of fungal necromass (Hawkins *et al*., 2023). Given the dominant role that AM fungal necromass plays in microbial necromass, we hypothesized that AM symbiosis would have a positive effect on the accumulation of MAOC fraction by enhancing the formation of fungal necromass C in the rhizosphere.

In this study, a pot experiment was conducted in a climate chamber using *Lythrum salicaria* L. (USDA, Natural Resource Conservation Service, 2001) as the host plant and *Archaeospora trappei* (Morton and Redecker, 2001; Spain, 2003) as the AMF inoculum. Using 16S rRNA sequencing, the effects of AM symbiosis on soil microbial community composition and functions were investigated. Confocal laser scanning microscopy and flow cytometry were employed to quantify microbial survival and physiological status, including cell viability, apoptosis, and necrosis, in the samples collected from bulk soil and rhizosphere soil under the AMF inoculation and non-inoculation treatments. Soil amino sugars were used as microbial biomarkers to determine soil microbial necromass C under different treatments with the help of gas chromatography-mass spectrometry (GC-MS) analysis.

MATERIALS AND METHODS

Soil sample, AMF inoculum, and host plants

The soil (0–30 cm deep) was sampled from the shore of Gaoyou Lake, Yangzhou, Jiangsu Province, China (32° 45′18″ N, 119°15′11″ E), representing the lake-wetland ecosystem with a typical subtropical monsoon climate. The soil is classified as an Inceptisol according to the USDA Classification System. The soil consisted of 44.1% sand, 20.6% silt, and 35.3% clay, with a soil pH of 6.8 (soil:H_2O = 1:5), a bulk density of 1.32 g cm^{-3}, organic C of 28.89 g kg^{-1}, total nitrogen (N) of 2.61 g kg^{-1}, and available phosphorus of 22.36 mg kg^{-1}. Detailed methods used for characterizing the soil properties are presented in Text S1 (see Supplementary Material for Text S1). Prior to the experiments, the soil was air-dried and sieved through a 2-mm mesh for further use.

The AMF inoculum, consisting of *Archaeospora trappei* spores (5–20 spores g^{-1}), mycelium, and plant root fragments mixed with dry soil, was obtained from the College of Resources and Environmental Sciences, Nanjing Agricultural University, China. There were approximately 60 propagules (infection unit) per one gram inoculum, including spores (*ca*. 16 g^{-1}), hyphae (*ca*. 40 g^{-1}), and colonized root fragments (*ca*. 3 g^{-1}). We selected this fungus species, because it has been reported to exhibit high tolerance to flooding conditions in wetlands (Xu *et al*., 2016) and form symbiotic associations with a wide range of wetland plants (Ali *et al*., 2019). *Lythrum salicaria* was selected as the host plant due to its ubiquity as a wetland plant and its confirmed AM status (Wang *et al*., 2018). The seeds of *L. salicaria*, purchased from Dadi Agriculture Co., Ltd., China, were surface-sterilized with 5% sodium hypochlorite solution for 10 min and then thoroughly rinsed with deionized water. Germination was then induced by placing the treated seeds on moist filter paper for one week (Qian *et al*., 2019).

Experimental design

The seed germination, plant preculture, and AMF inoculation experiments were conducted in a climate chamber at Hohai University, Nanjing, Jiangsu Province, China. In detail, the growth conditions of plants in the climate chamber were controlled at a temperature of 23.9 ± 0.5 °C, relative humidity of 73.3%, and lux light intensity of 15 000, with a daily light period of 12 h. Following a 7-d period of seed germination, *L. salicaria* seedlings were precultured in the rhizoboxes (inner size: 50 cm × 20 cm × 2 cm) for three months. After preculture, two treatments were established with three replicates, including the AMF inoculation (+AM) and non-inoculation (−AM) treatments. In the +AM treatment, 20 g of inoculum was added, replacing the same mass of soil around the root system without damaging roots in the rhizobox. Each rhizobox contained the sampled soil with a depth of 35 cm, equivalent to 2 100 cm^3 of soil. The soil was left unsterilized to preserve its original chemical properties and the natural microbial community. To establish the −AM treatment, 20 g of inoculum was sterilized before the addition. The inoculum was added at a depth of 0–10 cm in the rhizobox, and after six months, as the plant roots grew downward, soil samples were collected at a depth of 20–35 cm (Fig. S1, see Supplementary Material for Fig. S1). Therefore, the impact of 20 g of inoculum on soil sample collection was negligible. Soil moisture was maintained at 60% of the water-holding capacity through the addition of distilled water every 2 d using the gravimetric method (Wei *et al*., 2023). In the preculture and AMF inoculation experiments, *L. salicaria* plants were fertilized with 150 mL of 1/4 strength Hoagland solution per week (Gomez-Hermosillo *et al*., 2006).

The AMF inoculation experiment was maintained for 6 months from August 15, 2022 to February 14, 2023. At the end of the AMF inoculation experiment, the samples of roots, rhizosphere soil (RS), and bulk soil (BS) were collected. For RS collection, the soil loosely attached to the roots was shaken off, and the soil remaining adhered to the roots was collected (Somenahally *et al*., 2011; Sun *et al*., 2021). The BS was collected, after collecting RS, by homogenizing the soil (< 2 cm) that was away from the roots (Guan *et al*., 2020). Four types of soil samples were collected from RS and BS under the +AM and −AM treatments, labeled as RS+AM, BS+AM, RS−AM, and BS−AM, respectively. After collection, soil samples were frozen at −80 °C before further analyses.

Determination of root morphology and AMF colonization

The roots of *L. salicaria* free of soil were washed with deionized water, air-dried, and scanned with a scanner (Epson 1600, Epson, India). Based on the dry weights of leaves, shoots, and roots, the above- and belowground bimasses of plants were obtained. Subsequently, WinRHIZO version Pro 5.0 (Regent, Canada) was utilized to determine root morphological parameters, comprising total length, surface area, mean diameter, volume, and the number of tips.

Microscopic examination and the estimation of AMF colonization were carried out by trypan blue staining. Each root sample was cut into 40 root segments of approximately 1 cm in length. The root segments were immersed in 10% (weight/volume) KOH for 1 h at 90 °C in the water bath and then rinsed with deionized water 3 times (Phillips and Hayman, 1970). After being acidified with 2% (weight/volume) HCl solution for 40 min at 24 °C, the root segments were stained with 0.05% (weight/volume) trypan blue at 90 °C for 15 min in lactoglycerol (1:1:1 lactic acid, glycerol, and water) (Moukarzel *et al*., 2020). After staining, the root segments were immersed in lactoglycerol for 2 d at 24 °C to destain and were then viewed under a biological microscope (NE620, Nexcope, China) (Paymaneh *et al*., 2023). The frequency of mycorrhiza, intensity of mycorrhizal colonization, and arbuscule abundance were calculated to evaluate mycorrhizal colonization (Gucwa-Przepióra *et al*., 2013).

DNA extraction and Illumina MiSeq sequencing

Total soil DNA was extracted from each homogenized soil sample (0.20 g) with the E.Z.N.A.® soil DNA kit (Omega Bio-tek, USA) following the manufacturer's instructions. The quality and quantity of extracted DNA were determined by 1.0% agarose gel electrophoresis and a NanoDrop® ND-2000 spectrophotometer (Thermo Scientific Inc., USA). The 16S rRNA gene in the hypervariable V3–V4 regions was amplified with primer pairs 338F (5′-ACTCCTACGGGAGGCAGCAG-3′) and 806R (5′-GGACTACHVGGGTWTCTAAT-3′) using an ABI GeneAmp® 9700 polymerase chain reaction (PCR) thermocycler (ABI, USA), with details presented in Text S2 (see Supplementary Material for Text S2). The PCR product extracted from 2% agarose gel was purified using the AxyPrep DNA gel extraction kit (Axygen Biosciences, USA) according to the manufacturer's instructions and then quantified using a Quantus™ fluorometer (Promega, USA). Purified amplicons were used to construct a sequencing library using the NEXTFLEX® Rapid DNA-Seq kit and then paired-end sequenced on an Illumina MiSeq PE300 platform (Illumina, USA) following the standard protocols by Majorbio Bio-Pharm Technology Co., Ltd., China. The Illumina MiSeq sequence data sets have been available at the National Center for Biotechnology Information (NCBI) Sequence Read Archive under BioProject number PRJNA989761.

Confocal laser scanning microscopy and flow cytometry

Nycodenz density gradient separation was used to extract

microbial cells from the original soil samples (Macedo *et al*., 2022). The procedure of soil cell extraction with Nycodenz density gradient separation is available in Text S3 (see Supplementary Material for Text S3). The cell viability assessment was performed using the Calcein AM/PI cell viability/cytotoxicity assay kit (Beyotime Biotechnology, China). Soil cells (purified microbial cells from soil matrices) obtained through Nycodenz extraction were stained with calcein acetoxymethyl ester and propidium iodide in the dark for 30 min. Live cells were labeled with calcein acetoxymethyl ester (green fluorescence) and dead cells with propidium iodide (red fluorescence). The cell observation and imaging were performed by confocal laser scanning microscopy LSM 800 (Zeiss, Germany). To quantify the number of live and dead cells in the obtained fluorescence images, the open-source software ImageJ was used to convert fluorescence images to 32-bit grayscale images, and MATLAB (MathWorks, USA) was used to read the gray value of each pixel point and calculate the number of hotspots.

Apoptosis (a form of regulated cell death) and necrosis (a form of accidental cell death) are two cell death mechanisms that are impacted by the biochemical environment (Wang *et al*., 2001). The flow cytometry analysis was performed to quantify the proportions of necrotic and apoptotic cells using a cell apoptosis detection kit with Annexin V-mCherry and SYTOX Green (Beyotime Biotechnology, China). Following the methods described by Li *et al*. (2019) with minor modifications, cell samples were filtered through a 0.22-μm pore size filter to remove coarse particles that could cause clogging of the flow cytometer (Beckman Coulter, USA) and incubated with 194 μL Annexin V-mCherry binding buffer, 5 μL Annexin V-mCherry, and 10 μL SYTOX Green solution for 20 min in the dark. During this process, both apoptotic and necrotic cells were capable of being stained with Annexin V-mCherry, while only necrotic cells were stained with SYTOX Green. Stained cell samples were analyzed using a flow cytometer (Beckman Coulter), and data analysis was performed using FlowJo V10 (Tree Star Inc., USA).

SOC fractionation and microbial necromass C determination

Soil samples were physically fractionated using a size fractionation procedure (Craig *et al*., 2022). After being air-dried and sieved (2 mm), the soil was dispersed in 0.5% (weight/volume) sodium hexametaphosphate, shaken on a reciprocal shaker for 18 h, and washed through a 53-μm sieve. The fraction that passed through the sieve ($<$ 53 μm) was obtained as the mineral-associated organic matter (MAOM), while the fraction retained on the sieve ($>$ 53 μm) was obtained as the particulate organic matter (POM). Both POM and MAOM were oven-dried at 70 °C to constant weight. The dried samples were weighed and ground for further analysis. Two SOC fractions (MAOC and POC) are defined as the organic C in MAOM and POM, respectively. The contents of the two SOC fractions were determined with a TOC analyzer (Model 1030, OI Analytical, USA). Additionally, the contents of MAOC and POC in BS were measured based on the dry weights of MAOM, POM, and total soil.

As specific microbial biomarkers, soil amino sugars were determined to quantify soil microbial necromass C in the POC and MAOC fractions (Craig *et al*., 2022). Bacterial necromass C was calculated based on the concentration of muramic acid (MurA), which is uniquely produced by bacteria. Meanwhile, fungal necromass C was calculated based on the concentration of glucosamine (Glu), which mainly originates from fungi (Joergensen, 2018; Ni *et al*., 2020). Amino sugars in soil samples were extracted by acid hydrolysis, purified with myoinositol as an internal standard, and derivatized to aldononitrile acetates before GC/MS analysis. A TRACE^{TM} 1300 series gas chromatograph coupled with a TSQ 8000 Evo triple quadrupole mass spectrometer (Thermo Fisher Scientific, USA) was utilized to identify and quantify four amino sugars (MurA, Glu, galactosamine, and mannosamine). Detailed GC/MS conditions are presented in Text S4 (see Supplementary Material for Text S4). The contents of bacterial and fungal necromass C (BNC and FNC, respectively, μg g^{-1}) were calculated using the following aligns (Liang *et al*., 2019).

$$\mathrm{BNC} = \rho_{\mathrm{MurA}} \times 45 \tag{1}$$

$$\mathrm{FNC} = (C_{\mathrm{Glu}} - 2C_{\mathrm{MurA}}) \times 179.17 \times 9 \tag{2}$$

where ρ_{MurA} is the concentration of MurA in μg g^{-1}; C_{Glu} and C_{MurA} are the concentrations of Glu and MurA in mmol kg^{-1}, respectively; 45 and 9 are the conversion factors from MurA to BNC and Glu to FNC, respectively; and 179.17 is the molecular weight of Glu (g mol^{-1}).

Statistical analysis

All experimental data were presented as the means ± standard deviations ($n = 3$). Based on the results from Levene's test of homogeneity of variances, comparisons among different soil samples in soil bacterial alpha diversity were performed using a one-way analysis of variance (ANOVA) followed by Tukey's *post-hoc* test. The prediction of microbial metabolic and other ecologically relevant functions was conducted by the Functional Annotation of Prokaryotic Taxa (FAPROTAX) database (Louca *et al*., 2016). Functions related to C degradation in the root system were selected to analyze the effects of AMF inoculation on microbial communities in BS and RS. The operational taxonomic unit (OTU) co-occurrence network of soil bacterial communities

was constructed using the relative abundance of the high-abundance OTUs and by calculating the Pearson correlation. The co-occurrence edges were retained based on the absolute value of the Spearman correlation coefficient ($|r| \geqslant 0.6$ and significance at $P < 0.05$. The visualization of the network was achieved using Gephi 0.10.

Significant differences among different soil samples (*i.e.*, RS+AM, BS+AM, RS−AM, and BS−AM) in microbial physiological status, POC and MAOC contents, *etc*., were tested through a one-way ANOVA followed by Tukey's *post-hoc* test at $P < 0.05$. Differences between the +AM and −AM treatments in mycorrhizal colonization levels, root morphology, *etc*., were tested by Student's t-test at $P < 0.05$, $P < 0.01$, and $P < 0.001$. A two-way ANOVA was used to examine the effects of different soil samples and SOC fractions (POC and MAOC) on soil microbial necromass C. Analyses were performed utilizing IBM SPSS Statistics (version 22.0) or R (http://www.r-project.org/).

RESULTS

Effects of AMF inoculation on root morphology traits

After AMF inoculation, AM symbiosis was observed in the *L. salicaria* root system under the +AM treatment (Fig. 1a, c), with the frequency of mycorrhiza, intensity of mycorrhizal colonization, and arbuscule abundance reaching 72.50%, 36.23%, and 22.29%, respectively (Fig. 1e). Under the −AM treatment, AMF colonization was hardly detected in the root segments of *L. salicaria* root system, with the frequency of mycorrhiza less than 4% (Fig. 1d, e). Additionally, the belowground biomass of plants was significantly increased ($P < 0.05$) by AMF inoculation (Fig. 1f).

Root morphology parameters, total length, surface area, mean diameter, volume, and the number of tips, were significantly enhanced ($P < 0.05$) by AMF inoculation (Table I). Compared with *L. salicaria* roots under the −AM treatment, these root morphology parameters of *L. salicaria* under the +AM treatment increased by 27.96%, 30.00%, 50.00%, 45.77%, and 37.88%, respectively.

TABLE I

Root morphology traits of *Lythrum salicaria* under the arbuscular mycorrhizal fungi inoculation (+AM) and non-inoculation (−AM) treatments

Parameter[a)]	+AM	−AM
TL (cm)	559.73 ± 31.05[b)]**	437.44 ± 31.78
SA (cm^2)	128.49 ± 12.54*	98.84 ± 5.49
MD (cm)	0.33 ± 0.05*	0.22 ± 0.04
VL (cm^3)	4.65 ± 0.35**	3.19 ± 0.38
NTips	728 ± 50*	528 ± 96

*, **Significant differences between +AM and −AM treatments at $P < 0.05$ and $P < 0.01$, respectively.
[a)]TL = total length; SA = surface area; MD = mean diameter; VL = volume; NTips = number of tips.
[b)]Mean ± standard deviation ($n = 3$).

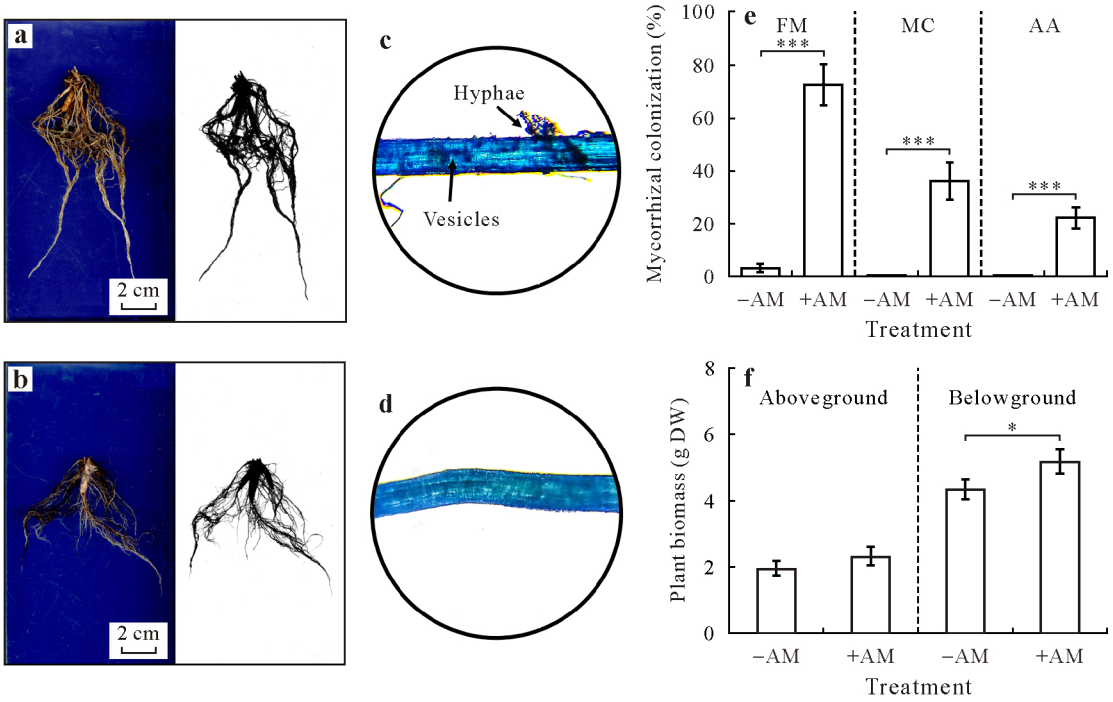

Fig. 1 Root systems and mycorrhizal colonization of *Lythrum salicaria* under the arbuscular mycorrhizal fungi inoculation (+AM) (a and c) and non-inoculation (−AM) (b and d) treatments, color and grayscale images of root systems (a and b), microscope photographs of mycorrhizal colonization in root system (c and d), and mycorrhizal colonization presented by frequency of mycorrhiza (FM), intensity of mycorrhizal colonization (MC), and arbuscule abundance (AA) (e), and above- and belowground biomasses of plants (f). Vertical bars indicate standard deviations of the means ($n = 3$). Asterisks * and *** indicate significant differences at $P < 0.05$ and $P < 0.001$, respectively.

Soil bacterial community composition and functions under +AM and −AM treatments

The number of raw sequence reads per soil sample ranged from 42 312 to 47 630, and the details of raw sequencing information are provided in Table SI (see Supplementary Material for Table SI). After removing single-end sequences without duplicates and OTU clustering of non-repetitive sequences (without single-end sequences) with a threshold of 97% similarity, a total of 332 760 representative sequences were obtained, and 4 145 OTUs were detected in 12 soil samples. The OTU rank-abundance curves indicated that RS+AM exhibited the highest bacterial species abundance and evenness (Fig. S2a, see Supplementary Material for Fig. S2). At the OTU level, RS+AM showed higher ($P < 0.05$) soil bacterial species diversity than other soil samples and exhibited the highest soil bacterial species richness (Fig. 2), consistent with the results of the OTU core and pan analysis (Fig. S2b, c).

As shown in Fig. 3a, RS+AM contained the greatest number of OTUs, totaling 3 495 OTUs. Additionally, the number of shared OTUs of the four types of soil samples was 2 387. At the phylum level, Proteobacteria, Firmicutes, Chloroflexi, and Actinobacteriota were the dominant phyla in the four types of soil samples (Fig. 3b). The AM symbiosis led to significant changes ($P < 0.01$) in the relative abundance of bacterial phyla, such as Proteobacteria, Firmicutes, and Actinobacteriota. Specifically, AMF inoculation resulted in an increase in the relative abundance of Proteobacteria in BS, rising from 25.1% in BS−AM to 29.0% in BS+AM, and in RS, rising from 27.7% in RS−AM to 28.4% in RS+AM. Compared with BS, the relative abundance of Firmicutes presented a downward trend in RS, from 20.4% in BS+AM to 16.2% in RS+AM and from 19.9% in BS−AM to 17.0% in RS−AM. Partial least squares-discriminant analysis (PLS-DA) illustrated that soil samples under the +AM treatment were separated from those under the −AM treatment, and bulk soil samples were separated from rhizosphere soil samples (Fig. S3, see Supplementary Material for Fig. S3). The effects of AM symbiosis on the characteristics of bacterial community in BS and RS were investigated using the co-occurrence network, which was constructed based on the relative abundance of bacteria with OTU level $> 0.1\%$ in BS+AM, BS−AM, RS+AM, and RS−AM and comprised 1 250 nodes, 3 583 edges, and 0.803 modularity (Fig. 3c). Under the +AM treatment, the rhizosphere soil (RS+AM *vs*. RS−AM) exhibited a higher richness of enriched OTUs (787) compared to the bulk soil (BS+AM *vs*. BS−AM), which contained 73 enriched OTUs, primarily associated with module 183 and module 100. Conversely, the rhizosphere soil (RS+AM *vs*. RS−AM) showed fewer depleted OTUs (92) than the bulk soil (BS+AM *vs*. BS−AM), which contained 149 depleted OTUs.

Fifty bacterial functions related to the C, N, and sulfur cycling were selected and predicted using FAPROTAX analysis (Fig. 4). The AMF inoculation affected soil nutrient metabolic processes in BS and RS, including hydrocarbon degradation, nitrate denitrification, nitrite denitrification, and sulfate respiration. To further explore the effect of AM symbiosis on soil C degradation, 7 relevant C degradation functions were selected, and the differences between the samples were examined (Fig. 5a, b). In RS, compared to RS−AM, RS+AM showed a significant increase ($P < 0.05$) in the relative abundance of functional microbial groups involved in cellulolysis and hydrocarbon degradation. In BS, compared to BS−AM, BS+AM exhibited a significant increase ($P < 0.05$) in the relative abundance of functional microbial groups involved in hydrocarbon degradation and aromatic hydrocarbon degradation.

Assessment of soil microbial physiological status in BS and RS

Dead microbial cells and cell fragments in soil are the primary contributors to soil microbial necromass accumulation. Based on confocal laser scanning microscopy images

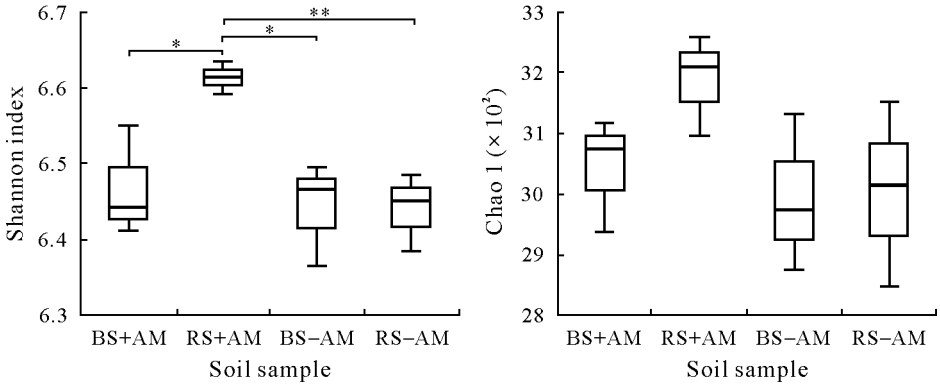

Fig. 2 Box plots of changes in bacterial within-community (alpha) diversity, *i.e*., species diversity (assessed by Shannon index) and richness (assessed by Chao 1), at the operational taxonomic unit level in the samples collected from bulk soil (BS) and rhizosphere soil (RS) under the arbuscular mycorrhizal fungi inoculation (+AM) and non-inoculation (−AM) treatments. Asterisks * and ** indicate significant differences at $P < 0.05$ and $P < 0.01$, respectively.

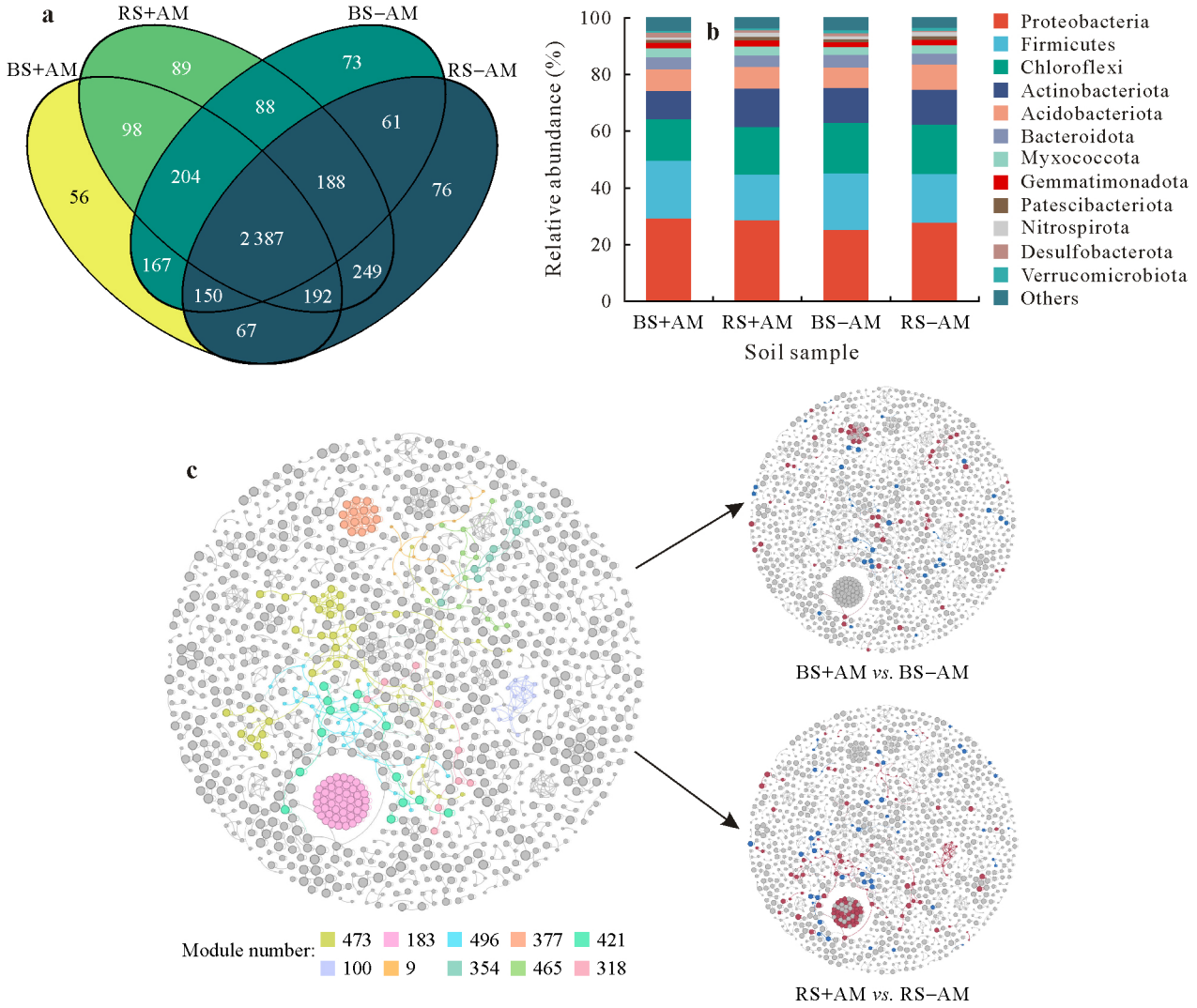

Fig. 3 Venn diagram of the shared and unique operational taxonomic units (OTUs) in bacterial communities (a), relative abundances of bacterial communities at the phylum level (b), and bacterial co-occurrence network (c) in the samples collected from bulk soil (BS) and rhizosphere soil (RS) under the arbuscular mycorrhizal fungi inoculation (+AM) and non-inoculation (−AM) treatments. Nodes within the co-occurrence network are assigned colors (red for enrichment and blue for depletion) based on the differential OTUs observed between samples BS+AM and BS−AM, as well as samples RS+AM and RS−AM.

of different soil samples (Fig. S4, see Supplementary Material for Fig. S4) and the estimation of the number of cells (Fig. 6a), the numbers of live and dead cells in RS+AM were significantly higher ($P < 0.05$) than those observed in the other soil samples. Only in the fluorescence images of RS+AM, the number of dead cells was observed to be higher than that of live cells, indicating that the proportion of dead cells in RS+AM was higher compared to the other soil samples. According to the flow cytometry analysis of different soil samples (Fig. S5, see Supplementary Material for Fig. S5), AM symbiosis significantly increased ($P < 0.05$) the proportions of necrotic and apoptotic cells in both BS and RS (Fig. 6b). Additionally, the proportions of necrotic and apoptotic cells were significantly higher ($P < 0.05$) in RS than in BS under the same treatment (Fig. 6b). In RS, the microbial death mode was dominated by apoptosis, whereas in BS, necrosis was the dominant mode of microbial death. Similar to the distribution of live and dead cells, the proportions of necrotic and apoptotic cells were the highest in RS+AM (12.15% and 19.02%, respectively) and the lowest in BS−AM (0.52% and 0.61%, respectively).

Distribution of MAOC and microbial necromass C contribution

Across all soil samples, RS+AM had the highest contents of POC (23.69 g kg^{-1} soil) and MAOC (17.20 g kg^{-1} soil), while BS−AM had the lowest contents of POC (20.47 g kg^{-1} soil) and MAOC (9.13 g kg^{-1} soil) (Fig. 7a). Positive effects of AM symbiosis were observed on the content of MAOC in RS. Following a pattern similar to the MAOC content across all soil samples, the proportion of MAOC was the highest in RS+AM (42.06%), and the lowest in BS−AM

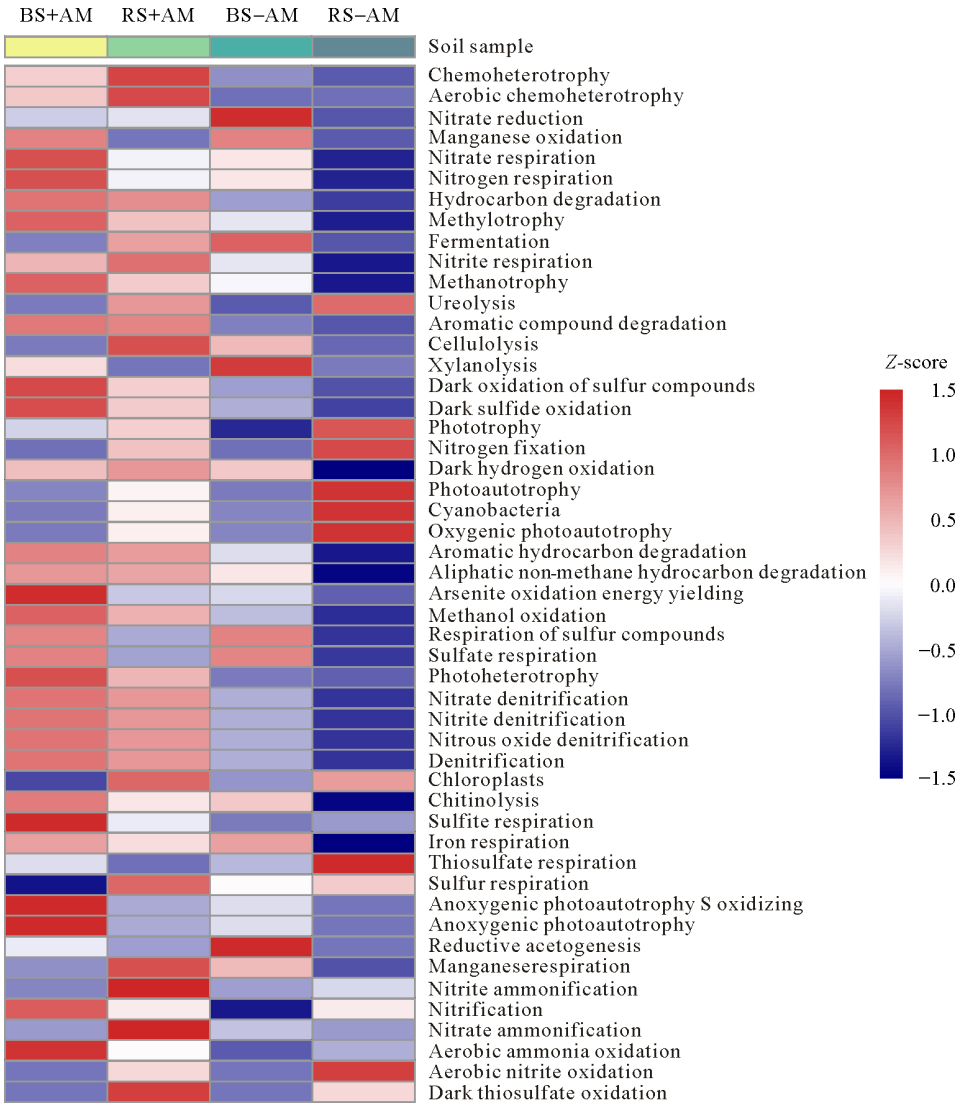

Fig. 4 Heatmap of potential bacterial functions related to N, C, and S cycling processes based on Functional Annotation of Prokaryotic Taxa (FAPROTAX) analysis in the samples collected from bulk soil (BS) and rhizosphere soil (RS) under the arbuscular mycorrhizal fungi inoculation (+AM) and non-inoculation (−AM) treatments. Different colors indicate relative abundances.

(30.83%) (Fig. 7b). To assess microbial contributions to POC and MAOC, the bacterial and fungal necromass C were calculated based on the amino sugar concentrations (Fig. S6, see Supplementary Material for Fig. S6). The concentrations of bacterial and fungal necromass C were significantly higher ($P < 0.001$) in the MAOC fraction than those in the POC fraction across all soil samples (Fig. 7c). The concentrations of bacterial (188.01 g kg^{-1} OC) and fungal (392.19 g kg^{-1} OC) necromass C in SOC fractions were found to be the highest in RS+AM, following a similar pattern to the MAOC content and proportion (Fig. 7c). Compared to bacterial necromass C, the concentration of fungal necromass C was significantly higher ($P < 0.001$) in different SOC fractions and in total soil (Fig. 7c, d), suggesting that fungal necromass C dominated the contribution of microbial necromass to the formation of MAOC and POC fractions. Specifically, AM symbiosis significantly promoted ($P < 0.05$) the concentrations of bacterial and fungal necromass C in the MAOC fraction and soil. The concentration of necromass C in soil presented the highest level (392.19 g kg^{-1} soil) in RS+AM.

DISCUSSION

Relationship between soil microbial community and MAOC proportion in rhizosphere soil

Here, we found that AM symbiosis modified the composition and function of soil microbial community. Our results illustrated that AM symbiosis significantly stimulated ($P < 0.05$) the relative abundance of functional microbial groups involved in hydrocarbon degradation in bulk and rhizosphere soils (Figs. 4 and 5). The extraradical mycelium

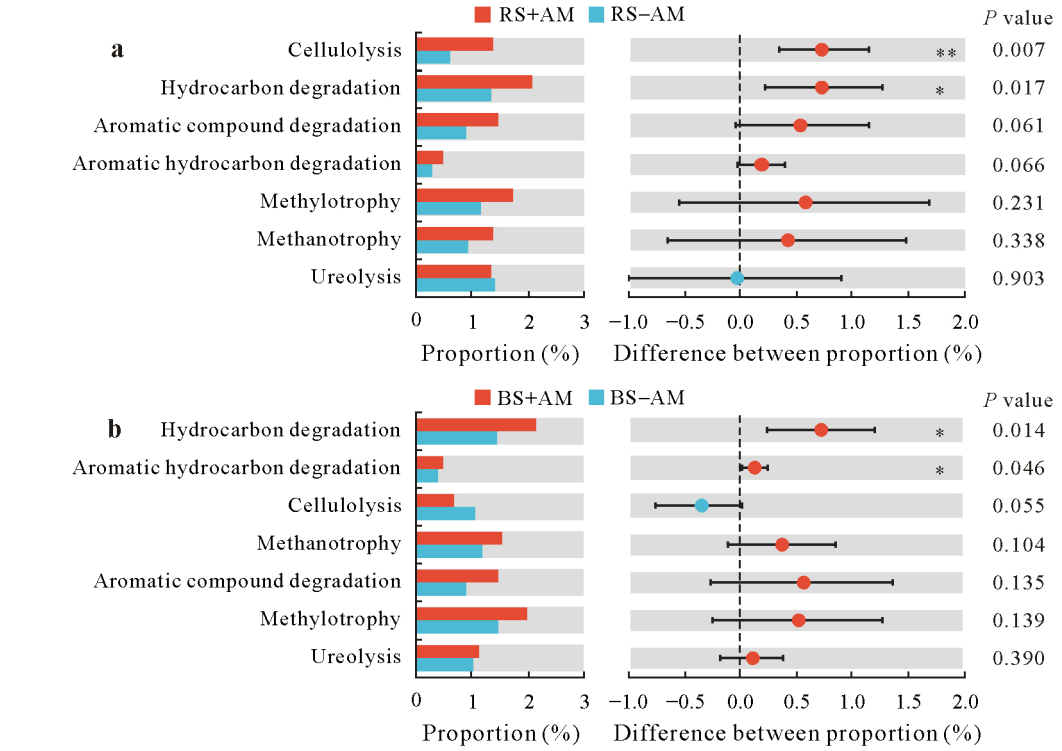

Fig. 5 Differences in bacterial C degradation-related functions between the samples collected from rhizosphere soil (RS) under the arbuscular mycorrhizal fungi inoculation (+AM) and non-inoculation (−AM) treatments (a) and between the samples collected from bulk soil (BS) under the +AM and −AM treatments (b). The horizontal bars indicate 95% confidence intervals. Asterisks * and ** indicate significant differences at $P < 0.05$ and $P < 0.01$, respectively.

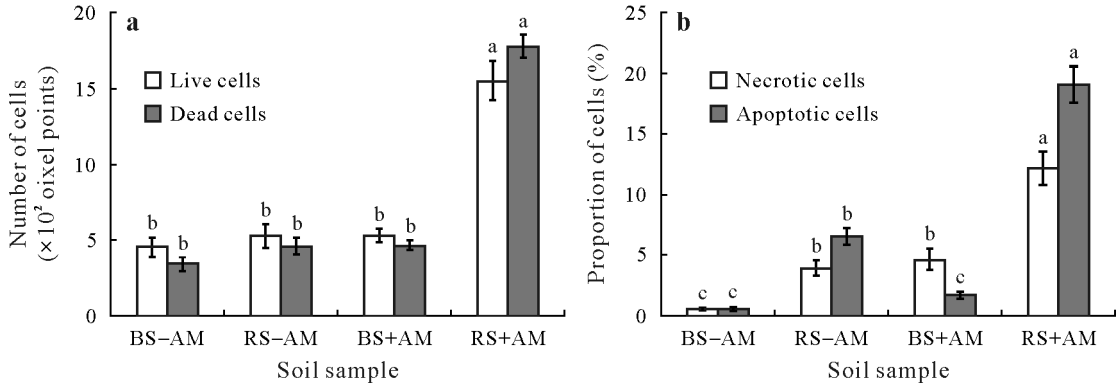

Fig. 6 Estimation of the numbers of live and dead cells based on confocal laser scanning microscopy images (a) and the proportions of necrotic and apoptotic cells based on Annexin V-mCherry/SYTOX Green flow cytometry analysis in the samples collected from bulk soil (BS) and rhizosphere soil (RS) under the arbuscular mycorrhizal fungi inoculation (+AM) and non-inoculation (−AM) treatment. Vertical bars indicate standard deviations of the means ($n = 3$). Different letters above bars for a given cell type indicate significant differences at $P < 0.05$.

of AMF beyond the rhizosphere could form the hyphosphere in bulk soil (Wang *et al*., 2022). The patterns of microorganisms in the hyphosphere were altered due to the release of hyphal exudates and the creation of a hyphosphere niche, including the degradative activity of the microorganisms in hydrocarbons (Qin *et al*., 2016; Rajtor and Piotrowska-Seget, 2016; Yuan *et al*., 2021). Our results confirmed that microbial functions related to C cycling processes were altered by AM symbiosis, including cellulose hydrolysis and aromatic compound degradation (Figs. 4 and 5). Consistent with our findings, microbial activities involved in the decomposition and consumption of exudates have been demonstrated to control the formation of MAOC by influencing the interaction between exudates and organic minerals in soil (Lei *et al*., 2023). Our study was limited to comparing rhizosphere and non-rhizosphere soils (bulk soils). Therefore, the effects of the hyphosphere in bulk soil, formed by the extraradical mycelium of AMF, on soil microbial community composition and functions remain unknown and require further investigation.

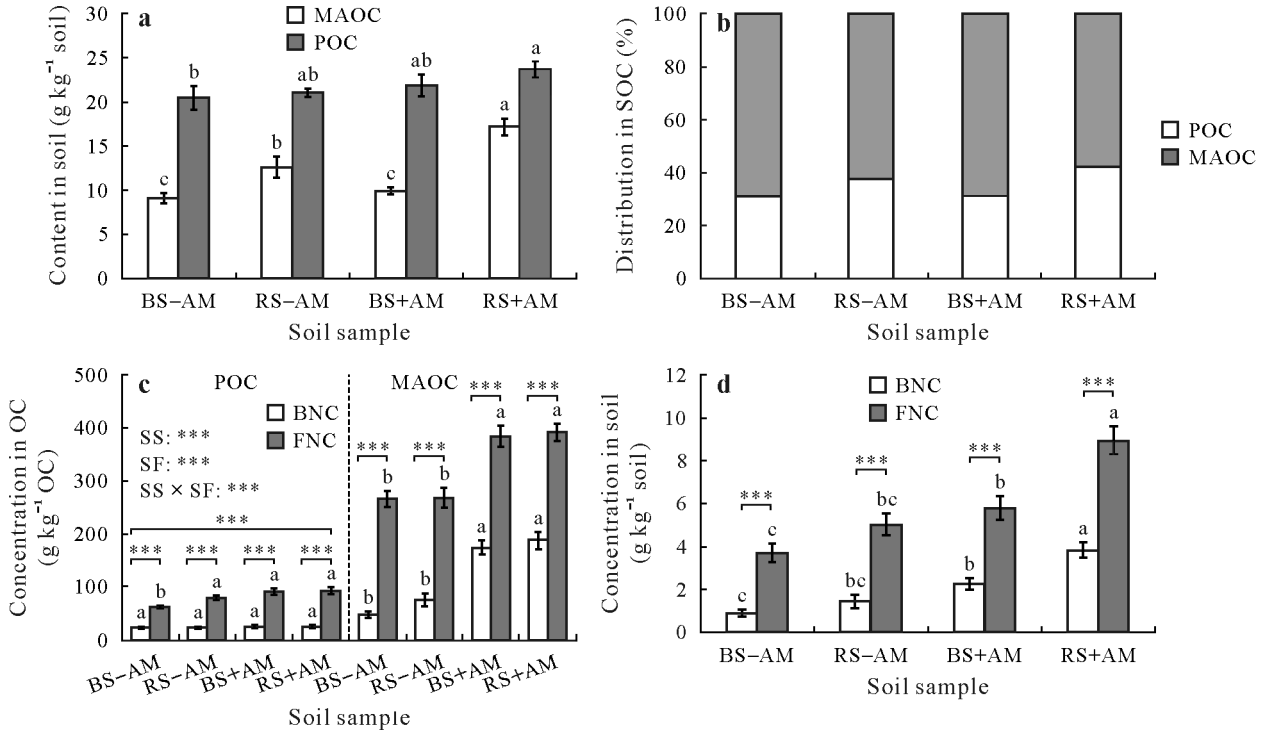

Fig. 7 Contents of soil mineral-associated organic C (MAOC) and particulate organic C (POC) (a), distributions of MAOC and POC in soil organic carbon (SOC) (b), concentrations of bacterial necromass C (BNC) and fungal necromass C (FNC) in soil POC and MAOC fractions (c), and soil BNC and FNC concentrations (d) in the samples collected from bulk soil (BS) and rhizosphere soil (RS) under the arbuscular mycorrhizal fungi inoculation (+AM) and non-inoculation (−AM) treatment. Vertical bars indicate standard deviations of the means ($n = 3$). Different letters above bars for a given organic C (OC) indicate significant differences at $P < 0.05$. Asterisks *** indicate significant differences or effects at $P < 0.001$. SS = soil sample; SF = SOC fraction; SS × SF = interaction of SS and SF.

Our results revealed that AM symbiosis significantly increased ($P < 0.05$) the MAOC content in rhizosphere soil, but not in bulk soil (Fig. 7a). Furthermore, we observed a higher proportion of MAOC in rhizosphere soil compared to bulk soil (Fig. 7b). In line with our findings, previous studies have argued that belowground plant root C inputs in rhizosphere exhibit a higher MAOC formation efficiency compared to aboveground litter C inputs (Keiluweit *et al*., 2015; Sokol and Bradford, 2019; Villarino *et al*., 2021). On one hand, it's widely acknowledged that the content of MAOC could be affected by the diversity and abundance of soil microbes (Luo *et al*., 2020; Wu *et al*., 2024). On the other hand, the diversity and abundance of soil microbes were reported to play an important role in the dynamics of SOC (Erktan *et al*., 2020). For example, the abundance ratio of bacterivores to fungivores positively correlates with the turnover of SOC (Jiang *et al*., 2018; Martin and Sprunger, 2021), and microbial diversity influences soil respiration and MAOC dynamics (Zhang and Zhang, 2016; Niu *et al*., 2024). Our study revealed a synchronous relationship between the POC and MAOC contents and proportions after a 6-month AMF inoculation experiment (Fig. 7). However, our experiments could not explore the dynamic impact of multi-year AMF inoculation on the distributions of POC and MAOC in soil. Thus, further study is required to explore the dynamics of POC and MAOC in soil by establishing long-term experiments.

More notably, AM symbiosis has been shown to change the quality and quantity of root and hyphal exudates, which could also affect soil microbial community and lead to increased release of plant C into the rhizosphere (Lioussanne *et al*., 2010; Zhang *et al*., 2012; Shahzad *et al*., 2015). Hence, although our study provided insight into soil bacterial community, soil microbial physiological status, and the distribution of MAOC under AM symbiosis, future research should focus on the effects of root and hyphal exudates mediated by AMF on soil microbial community, plant-derived C, and the distribution of POC.

Effects of AM symbiosis on soil microbial survival and physiological status in rhizosphere soil

Here, we found that AM symbiosis increased the number of soil microbial cells in rhizosphere soil regardless of live or dead cells (Fig. 6a). Synthesis studies have demonstrated that in the AM symbiosis system, both AM hyphae and plant roots release C-rich compounds into rhizosphere soil, and this process stimulates soil microbial growth and recruits distinct microbiomes in the rhizosphere (Zhang *et al*., 2016; Zhou *et al*., 2020). In previous studies, it has been reported that

AMF not only increase microbial biomass, but also accelerate microbial growth and turnover due to hyphal exudates, which contribute to SOC formation (Zhang L *et al*., 2022; Xu *et al*., 2023; Tao and Liu, 2024). To be specific, dissolved organic C present in root and hyphal exudates serves as the key substrate of soil microbes, and subsequently, necromass from these microbial cells becomes one of the pathways for the formation of MAOC in soil (Kakouridis *et al*., 2024). However, AMF not only promote the growth of soil microbes by feeding them with plant-derived C, but also suppress the abundance of certain soil microbes by absorbing significant amounts of nutrients from soil more efficiently, such as N and phosphorus (Veresoglou *et al*., 2012). For example, AMF suppress ammonia-oxidizing bacterial abundance by competing with them for free ammonium ions (Bukovská *et al*., 2018). The interactions between root symbiotic AMF and certain soil microbial groups are complex (Kiers *et al*., 2011; Zhang *et al*., 2014). Consistent with our study, microbial death pathways were found to determine the formation of microbial necromass C in soil (Camenzind *et al*., 2023). Dead cells, cell parts, cellular debris, and extracellular polymeric substances are all important components of microbial necromass (Wang C *et al*., 2023). Although confocal laser scanning microscopy could be used to qualitatively assess the number of dead cells, quantitative assessment of the number of dead cells, cell debris, and other decomposing products of microbial cells per unit of soil is still challenging.

We found that a higher proportion of soil microorganisms in bulk soil underwent the necrosis process rather than the apoptosis process (Fig. 6b). Soil microbial cell necrosis could occur by external injury such as pollutants addition and gamma sterilization (Wang *et al*., 2017; Dong *et al*., 2021), suggesting that the physiological status of soil microorganisms in bulk soil might be affected by environmental stress. It has been reported that microbial turnover is regulated by the production and death of microbial cells (Hagerty *et al*., 2014). Thus, the predominance of necrosis as the mode of microbial death implies that the turnover of microorganisms with AM symbiosis could be regulated by environmental conditions. In contrast, a greater proportion of soil microorganisms in rhizosphere soil underwent the apoptosis process rather than the necrosis process (Fig. 6b). As a form of regulated cell death, apoptosis is a natural and controlled physiological process (Li *et al*., 2019). This confirms that AM symbiosis constructs a C-rich environment in the rhizosphere and significantly accelerates the natural metabolism, growth, and death of rhizosphere soil microorganisms. From the assessment of soil microbial survival and physiological status under the +AM treatment, we demonstrate that AM symbiosis leads to a rise in the number of dead cells and the proportion of apoptotic cells, ultimately contributing to soil microbial turnover acceleration and soil necromass C accumulation in rhizosphere soil.

Fungal necromass C enriched by AM symbiosis and its contribution to MAOC accumulation

We observed a positive effect of AM symbiosis on microbial necromass accumulation (Fig. 7c). Consistent with our research, other studies have highlighted that AMF could not only stimulate the production of microbial necromass by accelerating microbial turnover, but also promote chemodiversity and the biochemical persistence of SOM (Wu *et al*., 2024; Yuan *et al*., 2024). In our study, the microbial necromass C concentration in the MAOC fraction was significantly higher than that in the POC fraction (Fig. 7c, d), highlighting the role of microbial necromass production in MAOC accumulation and SOC persistence, consistent with the findings from other studies (Luo *et al*., 2021; Wang B R *et al*., 2021b). It is worth mentioning that there are several methods to quantify the contribution of microbial necromass C, such as elemental C-N stoichiometry and biomarker scaling (Mooshammer *et al*., 2014). Nevertheless, direct quantification of microbial necromass C in soil remains elusive due to the complexity of distinguishing it from non-microbial organic C based on molecular signatures (Liang *et al*., 2019).

The proportion of fungal necromass C in both POC and MAOC fractions was significantly higher than that of bacterial necromass C (Fig. 7c). A higher contribution of fungal necromass was reported in the build-up of MAOC than bacterial necromass and plant residues (Klink *et al*., 2022). It has been reported that bacterial necromass biomarkers, represented by muramic acid, are more susceptible to decomposition compared to fungal necromass biomarkers (Chen *et al*., 2021). In addition, fungal hyphae can enhance the protection of fungal necromass by promoting soil aggregate formation, which potentially contributes to the higher concentration of fungal necromass C in SOC compared to bacterial necromass C (Hou *et al*., 2024). What's more, the living microbial biomass significantly impacts the contents of fungal and bacterial necromass C in soil, and a larger living fungal biomass, compared to bacterial biomass, could lead to a higher level of fungal necromass C (Wang B R *et al*., 2021a). Although we concluded that AM symbiosis had a great potential to promote MAOC formation by modulating microbial community composition and functions and increasing microbial necromass C input, especially fungal necromass C, the effects of AMF on the diversity of fungal community and the dynamics of fungal necromass C were not clear in our study. To better understand and quantify the fungal contribution to MAOC formation, further research should aim to identify and quantify specific microbiota, including both bacteria and fungi, that play a role in the formation and decomposition of necromass C under the influence of AM symbiosis.

CONCLUSIONS

This study found that AM symbiosis played a significant role in the accumulation of MAOC in the rhizosphere by promoting microbial contribution. Soil microbial community composition was analyzed by 16S rRNA sequencing, and microbial metabolic and other ecologically relevant functions were predicted by FAPROTAX analysis. The AM symbiosis significantly influenced the microbial community composition and increased soil microbial community functions related to C degradation. In terms of soil microbial survival and physiological status, AM symbiosis not only increased the number of soil microbial cells regardless of live and dead cells, but also enhanced the proportions of necrotic and apoptotic cells in the rhizosphere soil. With apoptosis as the dominant microbial death mode, soil microbial turnover could be accelerated, leading to the accumulation of soil necromass C in rhizosphere soil. Additionally, the concentration of fungal necromass C presented the highest level in the MAOC fraction in rhizosphere and bulk soils with AMF inoculation. In both POC and MAOC fractions, the concentration of fungal necromass C was significantly higher than that of bacterial necromass C, indicating the dominant contribution of fungal necromass C to MAOC accumulation in the rhizosphere soil. In conclusion, AM symbiosis increased the content and proportion of MAOC in rhizosphere soil by stimulating soil C degradation and increasing microbial necromass C input, especially fungal necromass C. Our study can assist in guiding the management of AMF application to produce positive impacts on MAOC formation and SOC sequestration.

DECLARATION OF COMPETING INTEREST

The authors declare that they have no known competing financial interests or personal relationships that could have appeared to influence the work reported in this paper.

ACKNOWLEDGEMENT

This study was supported by the National Natural Science Foundation of China (No. 51779078), the Six Talent Peaks Project in Jiangsu Province, China (No. JNHB-012), the National Major Projects of Water Pollution Control and Management Technology, China (No. 2017ZX07204003), and the Priority Academic Program Development (PAPD) of Jiangsu Higher Education Institutions, China.

SUPPLEMENTARY MATERIAL

Supplementary material for this article can be found in the online version.

REFERENCES

Adamczyk B, Sietiö O M, Biasi C, Heinonsalo J. 2019. Interaction between tannins and fungal necromass stabilizes fungal residues in boreal forest soils. *New Phytol*. **223**: 16–21.

Ali F, Jilani G, Fahim R, Bai L L, Wang C L, Tian L Q, Jiang H L. 2019. Functional and structural roles of wiry and sturdy rooted emerged macrophytes root functional traits in the abatement of nutrients and metals. *J Environ Manage*. **249**: 109330.

Averill C, Turner B L, Finzi A C. 2014. Mycorrhiza-mediated competition between plants and decomposers drives soil carbon storage. *Nature*. **505**: 543–545.

Bai Y F, Cotrufo M F. 2022. Grassland soil carbon sequestration: Current understanding, challenges, and solutions. *Science*. **377**: 603–608.

Bukovská P, Bonkowski M, Konvalinková T, Beskid O, Hujslová M, Püschel D, Řezáčová V, Gutiérrez-Núñez M S, Gryndler M, Jansa J. 2018. Utilization of organic nitrogen by arbuscular mycorrhizal fungi—Is there a specific role for protists and ammonia oxidizers? *Mycorrhiza*. **28**: 269–283.

Camenzind T, Mason-Jones K, Mansour I, Rillig M C, Lehmann J. 2023. Formation of necromass-derived soil organic carbon determined by microbial death pathways. *Nat Geosci*. **16**: 115–122.

Chari N R, Taylor B N. 2022. Soil organic matter formation and loss are mediated by root exudates in a temperate forest. *Nat Geosci*. **15**: 1011–1016.

Chen X B, Hu Y J, Xia Y H, Zheng S M, Ma C, Rui Y C, He H B, Huang D Y, Zhang Z H, Ge T D, Wu J S, Guggenberger G, Kuzyakov Y, Su Y R. 2021. Contrasting pathways of carbon sequestration in paddy and upland soils. *Glob Change Biol*. **27**: 2478–2490.

Cotrufo M F, Ranalli M G, Haddix M L, Six J, Lugato E. 2019. Soil carbon storage informed by particulate and mineral-associated organic matter. *Nat Geosci*. **12**: 989–994.

Cotrufo M F, Soong J L, Horton A J, Campbell E E, Haddix M L, Wall D H, Parton W J. 2015. Formation of soil organic matter *via* biochemical and physical pathways of litter mass loss. *Nat Geosci*. **8**: 776–779.

Cotrufo M F, Wallenstein M D, Boot C M, Denef K, Paul E. 2013. The Microbial Efficiency-Matrix Stabilization (MEMS) framework integrates plant litter decomposition with soil organic matter stabilization: Do labile plant inputs form stable soil organic matter? *Glob Change Biol*. **19**: 988–995.

Craig M E, Geyer K M, Beidler K V, Brzostek E R, Frey S D, Stuart Grandy A, Liang C, Phillips R P. 2022. Fast-decaying plant litter enhances soil carbon in temperate forests but not through microbial physiological traits. *Nat Commun*. **13**: 1229.

Dong W L, Song A L, Yin H Q, Liu X D, Li J W, Fan F L. 2021. Decomposition of microbial necromass is divergent at the individual taxonomic level in soil. *Front Microbiol*. **12**: 679793.

Erktan A, Rillig M C, Carminati A, Jousset A, Scheu S. 2020. Protists and collembolans alter microbial community composition, C dynamics and soil aggregation in simplified consumer-prey systems. *Biogeosciences*. **17**: 4961–4980.

Gomez-Hermosillo C, Pardue J H, Reible D D. 2006. Wetland plant uptake of desorption-resistant organic compounds from sediments. *Environ Sci Technol*. **40**: 3229–3236.

Guan X Y, Gao X Y, Avellan A, Spielman-Sun E, Xu J, Laughton S, Yun J, Zhang Y L, Bland G D, Zhang Y, Zhang R R, Wang X S, Casman E A, Lowry G V. 2020. CuO nanoparticles alter the rhizospheric bacterial community and local nitrogen cycling for wheat grown in a calcareous soil. *Environ Sci Technol*. **54**: 8699–8709.

Gucwa-Przepióra E, Błaszkowski J, Kurtyka R, Małkowski Ł, Małkowski E. 2013. Arbuscular mycorrhiza of *Deschampsia cespitosa* (Poaceae) at different soil depths in highly metal-contaminated site in southern Poland. *Acta Soc Bot Pol*. **82**: 251–258.

Hagerty S B, van Groenigen K J, Allison S D, Hungate B A, Schwartz E, Koch G W, Kolka R K, Dijkstra P. 2014. Accelerated microbial turnover but constant growth efficiency with warming in soil. *Nat Climate Change*. **4**: 903–906.

Hawkins H J, Cargill R I M, Van Nuland M E, Hagen S C, Field K J, Sheldrake M, Soudzilovskaia N A, Kiers E T. 2023. Mycorrhizal mycelium as a global carbon pool. *Curr Biol*. **33**: R560–R573.

Heckman K A, Possinger A R, Badgley B D, Bowman M M, Gallo A C, Hatten J A, Nave L E, SanClements M D, Swanston C W, Weiglein T L,

Wieder W R, Strahm B D. 2023. Moisture-driven divergence in mineral-associated soil carbon persistence. *Proc Natl Acad Sci USA*. **120**: e2210044120.

Hou Z N, Wang R H, Chang S, Zheng Y, Ma T T, Xu S Q, Zhang X J, Shi X, Lu J, Luo D Q, Wang B, Du Z L, Wei Y Q. 2024. The contribution of microbial necromass to soil organic carbon and influencing factors along a variation of habitats in alpine ecosystems. *Sci Total Environ*. **921**: 171126.

Jiang Y J, Zhou H, Chen L J, Yuan Y, Fang H, Luan L, Chen Y, Wang X Y, Liu M Q, Li H X, Peng X H, Sun B. 2018. Nematodes and microorganisms interactively stimulate soil organic carbon turnover in the macroaggregates. *Front Microbiol*. **9**: 2803.

Joergensen R G. 2018. Amino sugars as specific indices for fungal and bacterial residues in soil. *Biol Fert Soils*. **54**: 559–568.

Kakouridis A, Yuan M T, Nuccio E E, Hagen J A, Fossum C A, Moore M L, Estera-Molina K Y, Nico P S, Weber P K, Pett-Ridge J, Firestone M K. 2024. Arbuscular mycorrhiza convey significant plant carbon to a diverse hyphosphere microbial food web and mineral-associated organic matter. *New Phytol*. **242**: 1661–1675.

Keiluweit M, Bougoure J J, Nico P S, Pett-Ridge J, Weber P K, Kleber M. 2015. Mineral protection of soil carbon counteracted by root exudates. *Nat Climate Change*. **5**: 588–595.

Kiers E T, Duhamel M, Beesetty Y, Mensah J A, Franken O, Verbruggen E, Fellbaum C R, Kowalchuk G A, Hart M M, Bago A, Palmer T M, West S A, Vandenkoornhuyse P, Jansa J, Bücking H. 2011. Reciprocal rewards stabilize cooperation in the mycorrhizal symbiosis. *Science*. **333**: 880–882.

Kleber M, Eusterhues K, Keiluweit M, Mikutta C, Mikutta R, Nico P S. 2015. Mineral-organic associations: Formation, properties, and relevance in soil environments. *Adv Agron*. **130**: 1–140.

Klink S, Keller A B, Wild A J, Baumert V L, Gube M, Lehndorff E, Meyer N, Mueller C W, Phillips R P, Pausch J. 2022. Stable isotopes reveal that fungal residues contribute more to mineral-associated organic matter pools than plant residues. *Soil Biol Biochem*. **168**: 108634.

Kuyper T W, Jansa J. 2023. Arbuscular mycorrhiza: Advances and retreats in our understanding of the ecological functioning of the mother of all root symbioses. *Plant Soil*. **489**: 41–88.

Lange M, Eisenhauer N, Sierra C A, Bessler H, Engels C, Griffiths R I, Mellado-Vázquez P G, Malik A A, Roy J, Scheu S, Steinbeiss S, Thomson B C, Trumbore S E, Gleixner G. 2015. Plant diversity increases soil microbial activity and soil carbon storage. *Nat Commun*. **6**: 6707.

Lavallee J M, Soong J L, Cotrufo M F. 2020. Conceptualizing soil organic matter into particulate and mineral-associated forms to address global change in the 21st century. *Glob Change Biol*. **26**: 261–273.

Lei X, Shen Y T, Zhao J N, Huang J J, Wang H, Yu Y, Xiao C W. 2023. Root exudates mediate the processes of soil organic carbon input and efflux. *Plants*. **12**: 630.

Li H, Bölscher T, Winnick M, Tfaily M M, Cardon Z G, Keiluweit M. 2021. Simple plant and microbial exudates destabilize mineral-associated organic matter *via* multiple pathways. *Environ Sci Technol*. **55**: 3389–3398.

Li K, Qian J, Wang P F, Wang C, Fan X L, Lu B H, Tian X, Jin W, He X X, Guo W Z. 2019. Toxicity of three crystalline TiO_2 nanoparticles in activated sludge: Bacterial cell death modes differentially weaken sludge dewaterability. *Environ Sci Technol*. **53**: 4542–4555.

Li T T, Zhang J Z, Wang X, Hartley I P, Zhang J L, Zhang Y L. 2022. Fungal necromass contributes more to soil organic carbon and more sensitive to land use intensity than bacterial necromass. *Appl Soil Ecol*. **176**: 104492.

Liang C, Amelung W, Lehmann J, Kästner M. 2019. Quantitative assessment of microbial necromass contribution to soil organic matter. *Glob Change Biol*. **25**: 3578–3590.

Lioussanne L, Perreault F, Jolicoeur M, St-Arnaud M. 2010. The bacterial community of tomato rhizosphere is modified by inoculation with arbuscular mycorrhizal fungi but unaffected by soil enrichment with mycorrhizal root exudates or inoculation with *Phytophthora nicotianae*. *Soil Biol Biochem*. **42**: 473–483.

Louca S, Parfrey L W, Doebeli M. 2016. Decoupling function and taxonomy in the global ocean microbiome. *Science*. **353**: 1272–1277.

Lugato E, Lavallee J M, Haddix M L, Panagos P, Cotrufo M F. 2021. Different climate sensitivity of particulate and mineral-associated soil organic matter. *Nat Geosci*. **14**: 295–300.

Luo R Y, Luo J F, Fan J L, Liu D Y, He J S, Perveen N, Ding W X. 2020. Responses of soil microbial communities and functions associated with organic carbon mineralization to nitrogen addition in a Tibetan grassland. *Pedosphere*. **30**: 214–225.

Luo Y, Xiao M L, Yuan H Z, Liang C, Zhu Z K, Xu J M, Kuzyakov Y, Wu J S, Ge T D, Tang C X. 2021. Rice rhizodeposition promotes the build-up of organic carbon in soil *via* fungal necromass. *Soil Biol Biochem*. **160**: 108345.

Lv J T, Huang Z Q, Luo L, Zhang S Z, Wang Y W. 2022. Advances in molecular and microscale characterization of soil organic matter: Current limitations and future prospects. *Environ Sci Technol*. **56**: 12793–12810.

Macedo G, Olesen A K, Maccario L, Hernandez Leal L, van der Maas P, Heederik D, Mevius D, Sørensen S J, Schmitt H. 2022. Horizontal gene transfer of an IncP1 plasmid to soil bacterial community introduced by *Escherichia coli* through manure amendment in soil microcosms. *Environ Sci Technol*. **56**: 11398–11408.

Martin T, Sprunger C D. 2021. A meta-analysis of nematode community composition across soil aggregates: Implications for soil carbon dynamics. *Appl Soil Ecol*. **168**: 104143.

Mooshammer M, Wanek W, Zechmeister-Boltenstern S, Richter A. 2014. Stoichiometric imbalances between terrestrial decomposer communities and their resources: Mechanisms and implications of microbial adaptations to their resources. *Front Microbiol*. **5**: 22.

Morton J B, Redecker D. 2001. Two new families of Glomales, Archaeosporaceae and Paraglomaceae, with two new genera *Archaeospora* and *Paraglomus*, based on concordant molecular and morphological characters. *Mycologia*. **93**: 181–195.

Moukarzel R, Ridgway H J, Guerin-Laguette A, Jones E E. 2020. An improved clearing and staining protocol for evaluation of arbuscular mycorrhizal colonisation in darkly pigmented woody roots. *N Z Plant Protect*. **73**: 33–39.

Nahlik A M, Fennessy M S. 2016. Carbon storage in US wetlands. *Nat Commun*. **7**: 13835.

Ni X Y, Liao S, Tan S Y, Wang D Y, Peng Y, Yue K, Wu F Z, Yang Y S. 2020. A quantitative assessment of amino sugars in soil profiles. *Soil Biol Biochem*. **143**: 107762.

Niu Y L, Li Y, Lou M X, Cheng Z, Ma R J, Guo H, Zhou J, Jia H T, Fan L C, Wang T C. 2024. Microbial transformation mechanisms of particulate organic carbon to mineral-associated organic carbon at the chemical molecular level: Highlighting the effects of ambient temperature and soil moisture. *Soil Biol Biochem*. **195**: 109454.

Olsson P A, Rahm J, Aliasgharzad N. 2010. Carbon dynamics in mycorrhizal symbioses is linked to carbon costs and phosphorus benefits. *FEMS Microbiol Ecol*. **72**: 125–131.

Paymaneh Z, Sarcheshmehpour M, Mohammadi H, Askari Hesni M. 2023. Vermicompost and/or compost and arbuscular mycorrhizal fungi are conducive to improving the growth of pistachio seedlings to drought stress. *Appl Soil Ecol*. **182**: 104717.

Phillips J M, Hayman D S. 1970. Improved procedures for clearing roots and staining parasitic and vesicular-arbuscular mycorrhizal fungi for rapid assessment of infection. *Trans Brit Mycol Soc*. **55**: 158–161, IN16–IN18.

Qian J, Lu B H, Chen H, Wang P F, Wang C, Li K, Tian X, Jin W, He X X, Chen H. 2019. Phytotoxicity and oxidative stress of perfluorooctanesulfonate to two riparian plants: *Acorus calamus* and *Phragmites communis*. *Ecotox Environ Saf*. **180**: 215–226.

Qin H, Brookes P C, Xu J M. 2016. Arbuscular mycorrhizal fungal hyphae alter soil bacterial community and enhance polychlorinated biphenyls dissipation. *Front Microbiol*. **7**: 939.

Rajtor M, Piotrowska-Seget Z. 2016. Prospects for arbuscular mycorrhizal fungi (AMF) to assist in phytoremediation of soil hydrocarbon contaminants. *Chemosphere*. **162**: 105–116.

Shahzad T, Chenu C, Genet P, Barot S, Perveen N, Mougin C, Fontaine S. 2015. Contribution of exudates, arbuscular mycorrhizal fungi and litter depositions to the rhizosphere priming effect induced by grassland species. *Soil Biol Biochem*. **80**: 146–155.

Sokol N W, Bradford M A. 2019. Microbial formation of stable soil carbon is more efficient from belowground than aboveground input. *Nat Geosci*. **12**: 46–53.

Sokol N W, Sanderman J, Bradford M A. 2019. Pathways of mineral-associated soil organic matter formation: Integrating the role of plant carbon source, chemistry, and point of entry. *Glob Change Biol*. **25**: 12–24.

Somenahally A C, Hollister E B, Yan W G, Gentry T J, Loeppert R H. 2011. Water management impacts on arsenic speciation and iron-reducing bacteria in contrasting rice-rhizosphere compartments. *Environ Sci Technol*. **45**: 8328-8335.

Spain J L. 2003. Emendation of *Archaeospora* and of its type species, *Archaeospora trappei*. *Mycotaxon*. **87**: 109–112.

Sun Y P, Snow D, Walia H, Li X. 2021. Transmission routes of the microbiome and resistome from manure to soil and lettuce. *Environ Sci Technol*. **55**: 11102–11112.

Tao J Y, Liu X Y. 2024. Does arbuscular mycorrhizal fungi inoculation influence soil carbon sequestration? *Biol Fert Soils*. **60**: 213–225.

Terrer C, Phillips R P, Hungate B A, Rosende J, Pett-Ridge J, Craig M E, van Groenigen K J, Keenan T F, Sulman B N, Stocker B D, Reich P B, Pellegrini A F A, Pendall E, Zhang H, Evans R D, Carrillo Y, Fisher J B, Van Sundert K, Vicca S, Jackson R B. 2021. A trade-off between plant and soil carbon storage under elevated CO_2. *Nature*. **591**: 599–603.

United States Department of Agriculture (USDA), Natural Resource Conservation Service. 2001. PLANTS Database. Version 3.1. Available online at http://plants.usda.gov (verified on September 1, 2025).

van der Heijden M G A, Martin F M, Selosse M A, Sanders I R. 2015. Mycorrhizal ecology and evolution: The past, the present, and the future. *New Phytol*. **205**: 1406–1423.

Veresoglou S D, Chen B D, Rillig M C. 2012. Arbuscular mycorrhiza and soil nitrogen cycling. *Soil Biol Biochem*. **46**: 53–62.

Villarino S H, Pinto P, Jackson R B, Piñeiro G. 2021. Plant rhizodeposition: A key factor for soil organic matter formation in stable fractions. *Sci Adv*. **7**: eabd3176.

Wang B R, An S S, Liang C, Liu Y, Kuzyakov Y. 2021a. Microbial necromass as the source of soil organic carbon in global ecosystems. *Soil Biol Biochem*. **162**: 108422.

Wang B R, Liang C, Yao H J, Yang E, An S S. 2021b. The accumulation of microbial necromass carbon from litter to mineral soil and its contribution to soil organic carbon sequestration. *Catena*. **207**: 105622.

Wang C, Qu L R, Yang L M, Liu D W, Morrissey E, Miao R H, Liu Z P, Wang Q K, Fang Y T, Bai E. 2021. Large-scale importance of microbial carbon use efficiency and necromass to soil organic carbon. *Glob Change Biol*. **27**: 2039–2048.

Wang C, Wang X, Zhang Y, Morrissey E, Liu Y, Sun L F, Qu L R, Sang C P, Zhang H, Li G C, Zhang L L, Fang Y T. 2023. Integrating microbial community properties, biomass and necromass to predict cropland soil organic carbon. *ISME Commun*. **3**: 86.

Wang F, Zhang L, Zhou J C, Rengel Z, George T S, Feng G. 2022. Exploring the secrets of hyphosphere of arbuscular mycorrhizal fungi: Processes and ecological functions. *Plant Soil*. **481**: 1–22.

Wang F M, Lu X L, Sanders C J, Tang J W. 2019. Tidal wetland resilience to sea level rise increases their carbon sequestration capacity in United States. *Nat Commun*. **10**: 5434.

Wang J, Shu K H, Zhang L, Si Y B. 2017. Effects of silver nanoparticles on soil microbial communities and bacterial nitrification in suburban vegetable soils. *Pedosphere*. **27**: 482–490.

Wang J M, Silva J P, Gustafsson C M, Rustin P, Larsson N G. 2001. Increased *in vivo* apoptosis in cells lacking mitochondrial DNA gene expression. *Proc Natl Acad Sci USA*. **98**: 4038–4043.

Wang S G, Dai D W, Song S, Diao X J, Ma L M. 2018. Arbuscular mycorrhizal (AM) status in urban wetland plants and its impact factors. *Aquat Bot*. **150**: 33–45.

Wang Z G, Zhang Y Z, Govers G, Tang G P, Quine T A, Qiu J X, Navas A, Fang H Y, Tan Q, Van Oost K. 2023. Temperature effect on erosion-induced disturbances to soil organic carbon cycling. *Nat Climate Change*. **13**: 174–181.

Wei Z, Sixi Z, Xiuqing Y, Guodong X, Baichun W, Baojing G. 2023. Arbuscular mycorrhizal fungi alter rhizosphere bacterial community characteristics to improve Cr tolerance of *Acorus calamus*. *Ecotoxicol Environ Saf*. **253**: 114652.

Wu J L, Wu C F, Zhang Q, Zhang H Q, Wang S, Wang F, Jin S Q, Kuzyakov Y, Chen J P, Ge T D. 2024. Microbial diversity loss and wheat genotype-triggered rhizosphere bacterial and protistan diversity constrain soil multifunctionality: Evidence from greenhouse experiment. *Plant Soil*. **504**: 475–491.

Wu S L, Fu W, Rillig M C, Chen B D, Zhu Y G, Huang L B. 2024. Soil organic matter dynamics mediated by arbuscular mycorrhizal fungi—An updated conceptual framework. *New Phytol*. **242**: 1417–1425.

Xu Y J, Chen Z, Li X Y, Tan J, Liu F, Wu J P. 2023. The mechanism of promoting rhizosphere nutrient turnover for arbuscular mycorrhizal fungi attributes to recruited functional bacterial assembly. *Mol Ecol*. **32**: 2335–2350.

Xu Z Y, Ban Y H, Jiang Y H, Zhang X L, Liu X Y. 2016. Arbuscular mycorrhizal fungi in wetland habitats and their application in constructed wetland: A review. *Pedosphere*. **26**: 592–617.

Xue Z J, Qu T T, Li X Y, Chen Q, Zhou Z C, Wang B R, Lv X Z. 2024. Different contributing processes in bacterial *vs.* fungal necromass affect soil carbon fractions during plant residue transformation. *Plant Soil*. **494**: 301–319.

Yin L M, Dijkstra F A, Phillips R P, Zhu B, Wang P, Cheng W X. 2021. Arbuscular mycorrhizal trees cause a higher carbon to nitrogen ratio of soil organic matter decomposition *via* rhizosphere priming than ectomycorrhizal trees. *Soil Biol Biochem*. **157**: 108246.

Yuan M M, Kakouridis A, Starr E, Nguyen N, Shi S J, Pett-Ridge J, Nuccio E, Zhou J Z, Firestone M. 2021. Fungal-bacterial cooccurrence patterns differ between arbuscular mycorrhizal fungi and nonmycorrhizal fungi across soil niches. *mBio*. **12**: e03509-20.

Yuan Y S, Yin Y C, Adamczyk B, Liang D, Gu D P, Xia G W, Zhang J L, Zhang Z L. 2024. Nitrogen addition alters the relative importance of roots and mycorrhizal hyphae in regulating soil organic carbon accumulation in a karst forest. *Soil Biol Biochem*. **195**: 109471.

Zhang F G, Zhang Q G. 2016. Microbial diversity limits soil heterotrophic respiration and mitigates the respiration response to moisture increase. *Soil Biol Biochem*. **98**: 180–185.

Zhang G Y, Raza W, Wang X H, Ran W, Shen Q R. 2012. Systemic modification of cotton root exudates induced by arbuscular mycorrhizal fungi and *Bacillus vallismortis* HJ-5 and their effects on *Verticillium* wilt disease. *Appl Soil Ecol*. **61**: 85–91.

Zhang L, Fan J Q, Ding X D, He X H, Zhang F S, Feng G. 2014. Hyphosphere interactions between an arbuscular mycorrhizal fungus and a phosphate solubilizing bacterium promote phytate mineralization in soil. *Soil Biol Biochem*. **74**: 177–183.

Zhang L, Xu M G, Liu Y, Zhang F S, Hodge A, Feng G. 2016. Carbon and phosphorus exchange may enable cooperation between an arbuscular mycorrhizal fungus and a phosphate-solubilizing bacterium. *New Phytol*. **210**: 1022–1032.

Zhang L, Zhou J C, George T S, Limpens E, Feng G. 2022. Arbuscular mycorrhizal fungi conducting the hyphosphere bacterial orchestra. *Trends Plant Sci*. **27**: 402–411.

Zhang Z L, Kaye J P, Bradley B A, Amsili J P, Suseela V. 2022. Cover crop functional types differentially alter the content and composition of soil organic carbon in particulate and mineral-associated fractions. *Glob Change Biol*. **28**: 5831–5848.

Zhou J C, Chai X F, Zhang L, George T S, Wang F, Feng G. 2020. Different arbuscular mycorrhizal fungi cocolonizing on a single plant root system recruit distinct microbiomes. *mSystems*. **5**: e00929-20.